Torsten Leutbecher	***Ekkehard Fehling***
Dr.-Ing.	***Prof. Dr.-Ing.***
IBB Fehling + Jungmann	***Kassel University, Institute of Structural Engineering***
Kassel, Germany	***Kassel, Germany***

Crack Formation and Tensile Behaviour of UHPC Reinforced with a Combination of Rebars and Fibres

Summary

To carry tensile loads beyond the tensile strength of fibre reinforced UHPC in beams or tensile members, fibres can be combined with conventional bar reinforcement or prestressing steel. Thereby, the structural and deformation behaviour in serviceability as well as in ultimate limit state is affected significantly. Based on equilibrium and compatibility, the introduced mechanical model enables to predict both the integral load-deformation-behaviour and the width of discrete cracks of UHPC-tensile members reinforced with rebars and fibres. Fundamentals are the well-known mechanical principles for cracked reinforced concrete and the stress-crack-opening-relationship of fibre concrete. The application of the proposed model to an extensive test series with numerous varied parameters shows a very good agreement even for fibre-reinforced UHPC with strain softening behaviour.

Keywords: *tensile behaviour, combined reinforcement, crack width, durability, economic mix design*

1 Introduction

To achieve ductile post failure behaviour in compression and to increase tensile strength and ductility of UHPC, often fibres, normally high strength steel fibres, are added. Thus very high flexural strengths can be achieved, particularly for thin structural members. However, to realise long-span structures (i. e. bridges) under systematic utilisation of the high compressive strength of concrete, additional untensioned or prestressed reinforcement in the tensile area is needed.

Thereby, differences in the load bearing and the deformation behaviour compared to common reinforced concrete and prestressed concrete result from the interaction of continuous reinforcement elements and discontinuously distributed short fibres. In particular stiffness and cracking, but also bearing capacity and ductility, are significantly affected by the reinforcement configuration.

The calculation of UHPC structures therefore requires methods and models, which describe the mechanical processes of cracking well and thus enable a material suited structural design. In order to ensure durability, a secure limitation of crack width in serviceability state plays an important role.

2 Bond between UHPC and bar reinforcement

Within a test series, the bond between rebars (BSt 500, high strength ribbed prestressing steel St 1420/1570 and St 1470/1620) with different diameters (d_s = 8, 10 and 12 mm) and fine-aggregate UHPC of mixture M1Q (table 1) was investigated experimentally. Depending on the fibre content the compressive strengths of the UHPC-mixture lie between 160 and 190 N/mm².

Table 1: UHPC-mixture [1]

UHPC-mixture		**M1Q**	**M2Q**
cement	kg/m³	733	832
sand 0.125/0.50	kg/m³	1008	975
silica fume	kg/m³	230	135
fine quartz	kg/m³	183	207
finest particles < 0.125 mm	l/m³	405	403
superplasticiser	kg/m³	28.6	29.4
water	l/m³	161	166
water-cement-ratio		0.24	0.22
water-binder-ratio		0.19	0.19

Differing from the recommendations of RILEM [2], for the pull-out-tests' specimens the bond length was reduced to 1.5 d_s, to avoid yielding of reinforcing steel. Besides concrete cubes with edge lengths of 10 d_s specimens with reduced concrete cover (2.5 and 1.0 d_s) were tested. Furthermore, the influence of steel fibres (l/d = 17 mm/0.15 mm) was investigated.

The highest bond strength was reached for BSt 500 with a concrete cover of 4.5 d_s at comparatively small relative displacements of about 0.1 to 0.2 mm (figure 1). High strength steel with indentation showed definitely softer bond behaviour. For reduced concrete cover of 2.5 d_s longitudinal cracks along the reinforcing steel bar caused a reduction of bond strength. This could not be avoided even by adding fibres of 1.0 vol.-%.

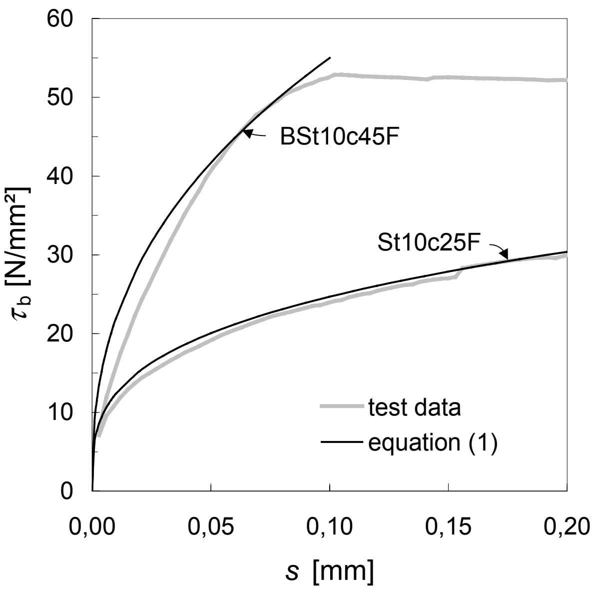

BSt10c45F = BSt 500, Ø 10 mm, concrete cover: 45 mm, 1.0 vol.-% steel fibres

St10c25F = St 1420/1570, Ø 10 mm, concrete cover: 25 mm, 1.0 vol.-% steel fibres

Figure 1: Bond behaviour of reinforcing steel (BSt 500) and high strength ribbed prestressing steel (St 1420/1670) in fibre reinforced fine-aggregated UHPC (grey) and approximation by equation (1) (black)

As bond law for reinforced NSC equation (1) is used frequently. Fitting the input parameters, the bond behaviour of UHPC can be approximated by equation (1) as well (figure 1). Table 2 represents the parameters based on the results of the conducted pull-out-tests.

$$\tau_b = \tau_{b\,max} \cdot \left(\frac{s}{s_1}\right)^{\alpha} \leq \tau_{b\,max} \qquad (1)$$

with $\tau_{b\,max}$ bond strength
s slip
s_1 slip at reaching the bond strength
α constant, depending on the bond quality of the reinforcing steel

Table 2: Parameters to describe the bond behaviour of UHPC by equation (1)

type of reinforcement		BSt 500	St 1420/1670
$\tau_{b\,max}$	N/mm²	55	40
s_1	mm	0.1	0.5
α	-	0.40	0.30

3 Stress-crack-opening-relationship of fibre reinforced UHPC

For fine-aggregate UHPC of mixture M2Q (table 1), the stress-crack-opening-behaviour was investigated experimentally within a test series on notched prisms. Smooth high strength steel fibres with a diameter of 0.15 mm and a length of 9 mm or 17 mm were added to the concrete in different volume fractions (0.9 up to 2.5 vol.-%). The prisms had a cross section of 40 x 40 mm² with 5 mm x 5 mm sawn notches at two opposite sides (figure 2).

To avoid failure outside the notch and to enable the measurement of very small values of crack opening, thin steel plates, which reached directly to the notch edge, were glued to the lateral surface of the test specimens. The chosen load application per threaded bars without hinges led to an elastic restraint of the specimens (figure 3).

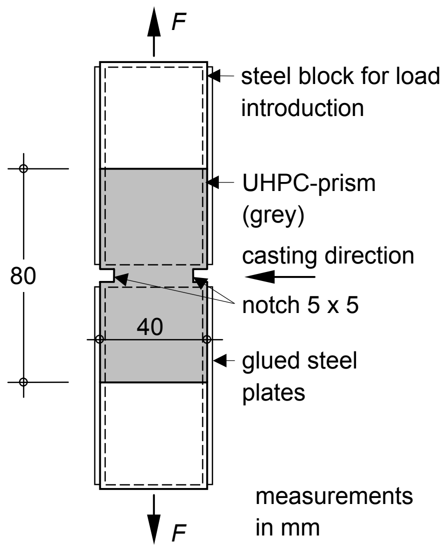

Figure 2: Test specimen

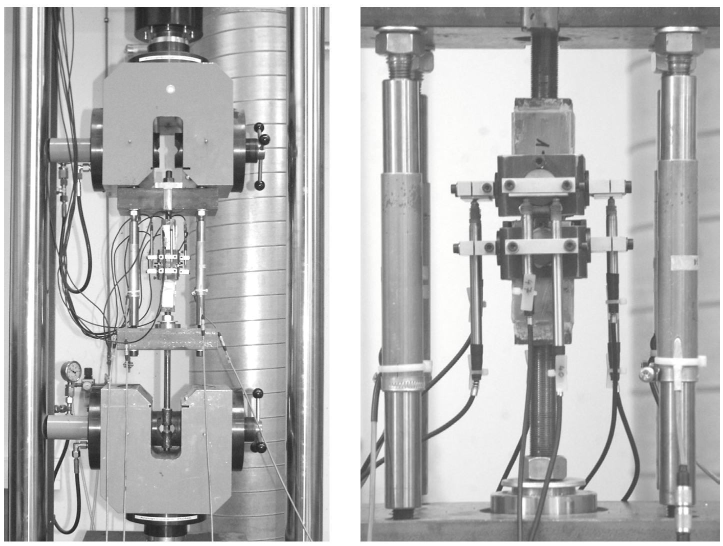

Figure 3: Test set-up (left) and instrumentation (right)

The deformations were measured by LVDT's, which were fastened at the steel plates by a device near to the notch edge. Figure 4 shows the obtained stress-crack opening-relationships. They can be approximated very well in the phase of both, fibre activation (figure 4a) and fibre pull-out (figure 4b) by the following equations, as given among others by Pfyl [3].

fibre activation: $\sigma_{cf} = \sigma_{cf0} \cdot \left(2\sqrt{\frac{w}{w_0}} - \frac{w}{w_0} \right)$ (2a) fibre pull-out: $\sigma_{cf} = \sigma_{cf0} \cdot \left(1 - \frac{2w}{l_f} \right)^2$ (2b)

with σ_{cf0} maximum stress of fibre concrete (post-cracking phase)
w_0 crack width at reaching the maximum stress of fibre concrete
l_f fibre length

To consider the influence of shrinkage and of matrix-softening in the state of micro cracking, the equations (2a) and (2b) can be extended as shown in [4].

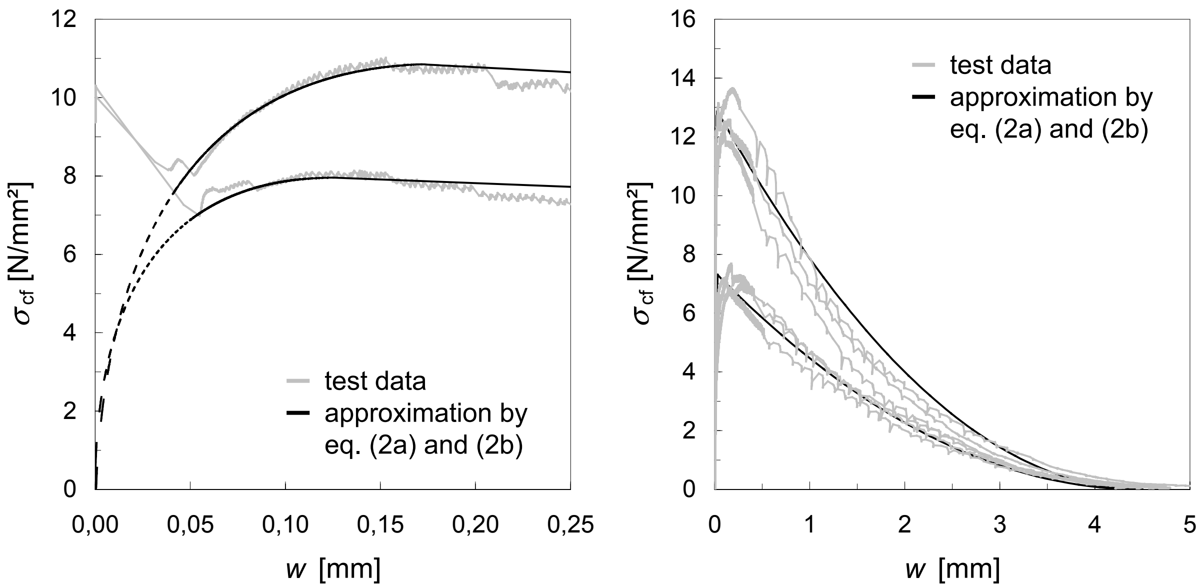

Figure 4: Stress-crack opening-relationship in the fibre activation phase (left, 17 mm long steel fibres) and until complete pull-out of all fibres (right, 9 mm long steel fibres)

4 Tensile behaviour of UHPC reinforced with rebars and fibres

4.1 Mechanical model

To describe the tensile behaviour of tensile members with a combination of bar and fibre reinforcement, the mechanical relationships valid for fibre concrete and reinforced concrete have to be linked. For balance reasons, within the crack equation (3) is true. In the state of micro cracking, equation (3) may be extended by the contribution of the UHPC-matrix F_c.

$F = F_s + F_f$ (equilibrium condition) (3)

with F external tensile force
F_s tensile force of reinforcing bars
F_f tensile force of fibres

Implying plane cross sections, the relative displacement between bar reinforcement and matrix on one hand and the stress-crack-opening-relationship of fibre concrete on the other hand must lead to identical crack widths (compatibility condition). Considering the equilibrium condition and the compatibility condition, the tensile forces of bar and fibre reinforcement and therewith the local as well as the integral strain of an UHPC-tensile member with combined reinforcement can be determined definitely.

As shown in [4], with increasing bond stress between concrete and reinforcement acc. to figure 1 and with further fibre activation (figure 2a) new cracks can arise up to high elastic tensile strain. At this, the fibre concrete itself does not need to show a strain hardening behaviour.

Because of the quite complex mechanical relationships, the iterative evaluation of the equilibrium and compatibility conditions has to be done numerically. In the proposed model the tensile member is divided into a finite number of "crack elements" of discrete lengths. These elements differ in the fibre content effective in tensile direction (considering the scatter of fibre distribution and orientation) and in their length. The lengths of the elements measure the single up to the twice of the load transition length of the bar reinforcement (possible crack spacings in the state of single cracking), which shows a more unfavourable bond behaviour compared to the fibres.

The calculation of the load-deformation-behaviour of the different elements is conducted force-controlled. Therefore, the external load is increased incrementally, starting with the smallest cracking strength of all considered crack elements. On each load level, the internal forces, the crack width, the average tensile strain etc. are determined by iteration for all crack elements. It is checked, if in the middle of two existing cracks the cracking strength of fibre concrete is reached again. In this case for the next load level the crack spacing is halved and the number of cracks of the corresponding element is doubled. Subsequently, for each load level a statistical evaluation (frequency distribution of the crack spacings and crack widths, extreme and mean values etc.) and the superposition of the average steel strain values is done. Thereby the results of the elements are weighed according to their distribution density.

4.2 Experimental verification of the proposed mechanical model

4.2.1 Test programme and test execution

To analyse the interaction of bar and fibre reinforcement, tensile tests on panel-shaped UHPC-members (mixture M2Q acc. to table 1) have been carried out. Within the test series the influence of the fibre length (9 and 17 mm), of the fibre content (0.9 up to 2.5 vol.-%), of the type of bar reinforcement (BSt 500, high strength steel, see figure 1), of the bar diameter (8 and 12 mm) and of the content of bar reinforcement (1.3 and 3.0 %) on the load and deformation behaviour under short-term monotonic loading was investigated.

The panels had a cross section of 70 x 220 mm² and a length of 1300 mm (figure 5). They were reinforced in tension direction concentrically with one layer of 4 steel bars each. Some specimens had an additional lateral reinforcement. The panels were implemented by clamp jaws in a servo-hydraulic test device (figure 6). The loading was conducted path controlled.

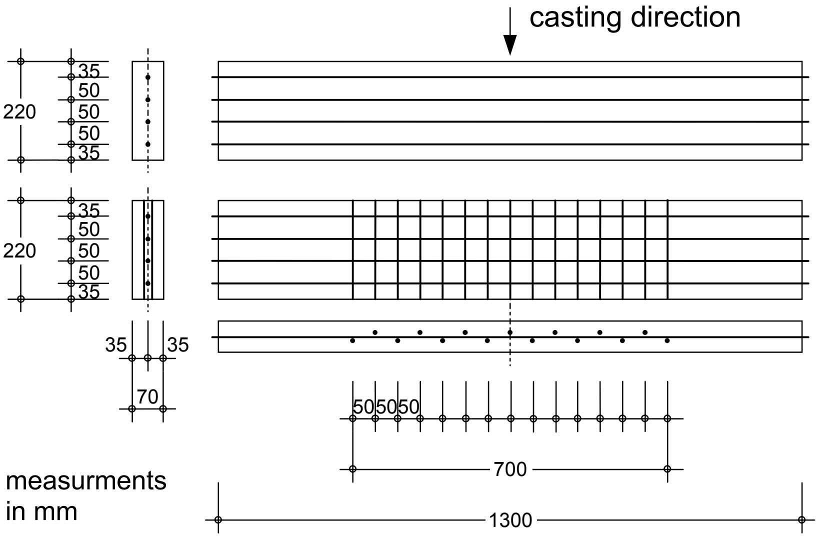

Figure 5: Dimensions and reinforcement of UHPC-panels

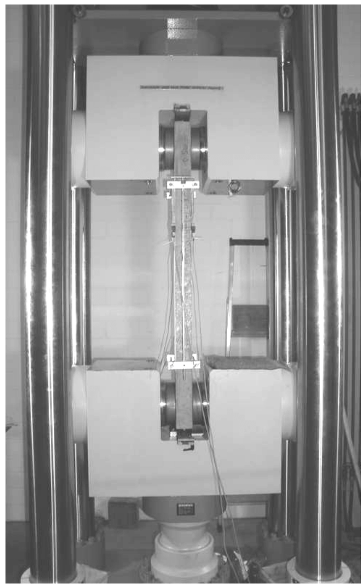

Figure 6: Test setup

The deformations were measured integrally by 4 LVDT's over a measuring range of 750 mm. Crack formation and development of crack width were observed visually via crack loupe at discrete strain states. Furthermore, results about the crack width distribution should be gained indirectly through the correlation between crack width and crack spacing. Therefore, the crack spacings were measured on the front and back side along 3 measuring ranges each.

4.2.2 Shortening due to shrinkage

Due to the high cement content and the low water-binder-ratio of UHPC the autogenous shrinkage exceeds the drying shrinkage. According to tests done by Fehling et al. [1] with mixture M1Q, the autogenous shrinkage strain ε_{cas} amounts to about 0.9 ‰. Considering the minor drying shrinkage strain ε_{cds} the total degree of total shrinkage $\varepsilon_{cs\infty}$ sums up to approximately 1 ‰.

Within the test series, the shortening due to shrinkage $\varepsilon_{s,shr}$ was determined experimentally. For that purpose the length of the reinforcement bars, which stick out at the ends of the panels, were measured before being implemented in the formwork and another time several days after finishing the heat treatment of the hardened specimens. Figure 7 shows the measured shrinkage shortening as a function of the total reinforcement ratio ρ_{tot}. The fibre content is considered by half in comparison to the bar reinforcement ratio.

Equation (4) describes the theoretical $\varepsilon_{s,shr}$ - ρ_{tot} -relationship. The unknown parameters can be determined via regression analysis using the measured values (broken line in figure 7).

$$\varepsilon_{s,shr} = \frac{\varepsilon_{cs\infty}}{1 + \alpha_E \cdot \rho_{tot} \cdot (1 + \rho \cdot \varphi)} \tag{4}$$

with φ creep coefficient

ρ relaxation coefficient

$\alpha_E = E_s / E_c$

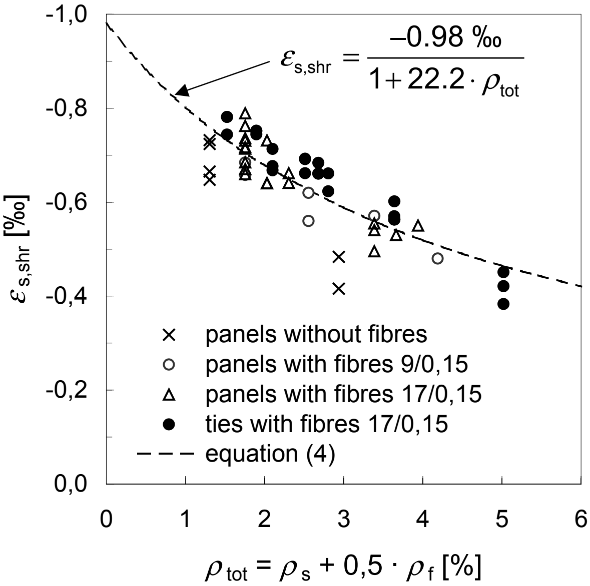

Figure 7: Shortening of tensile members due to shrinkage

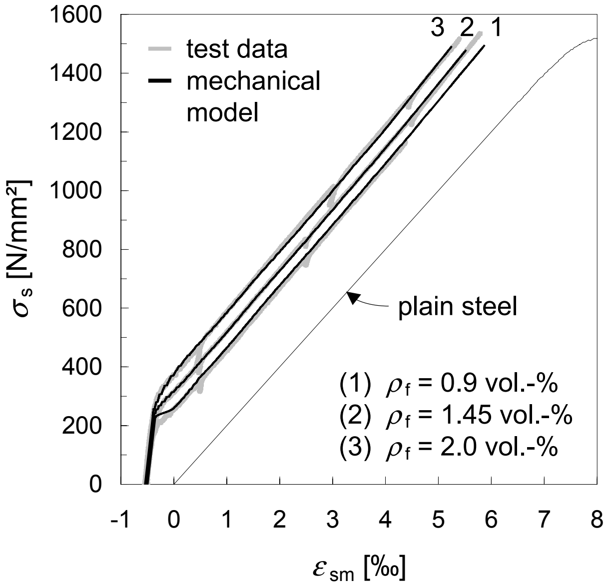

Figure 8: Load-deformation-behaviour of tensile members (high strength steel, d_s = 12 mm and 17 mm long fibres)

4.2.3 Load-deformation-behaviour and crack formation

Figure 8 shows the stress-strain-relationships obtained by the tensile tests. The average strain ε_{sm} was calculated from the displacements measured by the 4 LVDT's and the shrinkage shortening acc. to figure 7. A very good agreement with the proposed model is achieved.

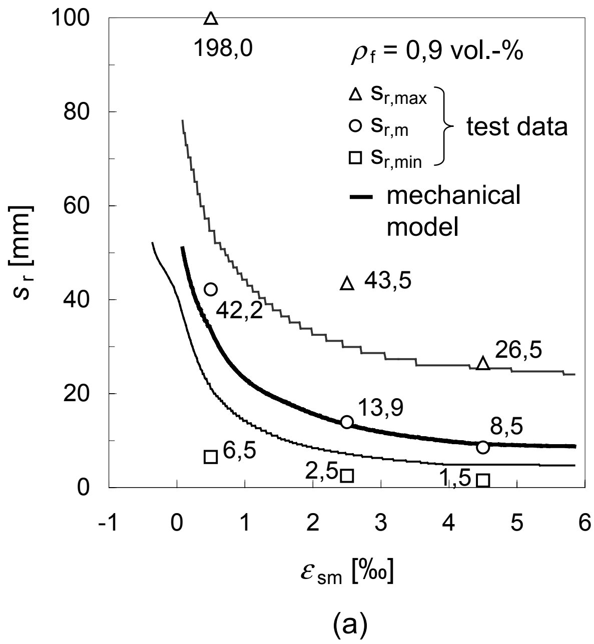

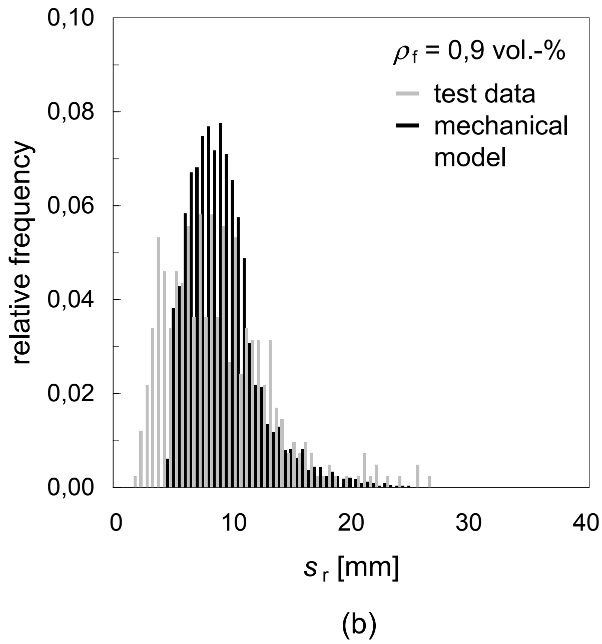

Figure 9: Development of crack spacings during tests (a) and relative frequency distribution of the crack spacings at the end of tests (b) in comparison to the mechanical model (high strength steel, d_s = 12 mm and 17 mm long fibres)

In figure 9a, the maximum, minimum and mean values of crack spacings are depicted numerically and by symbols. They were obtained by the analysis of recorded test data for the specimens with a fibre content of 0.9 vol.-%. Figure 9b shows the relative frequency distribution of crack spacing at the end of tests as histogram (grey bars).

The calculation by the mechanical model is based on the same material parameters as the calculation of the load-deformation-behaviour. Again, an overall very good agreement between test data and mechanical model could be obtained. Due to the assumption of plain cross sections (Bernoulli's hypothesis), the minimum crack spacings, measured in the tests, which may emerge near to crack splittings, are overestimated by the model.

5 Conclusions

The load-deformation-behaviour as well as the development of crack spacings and crack widths observed in the tests can be represented very well by the suggested mechanical model [4]. The calculations are based on the bond-stress-slip-relationships of bar reinforcement and on the stress-crack-opening-relationships of ultra high strength fibre concrete. Thus, the introduced model enables both calculations of stiffness and of crack widths of non-prestressed reinforced as well as prestressed UHPC-tensile members.

Experimental and theoretical studies show, that the tension stiffening effect increases strongly with increasing fibre, but crack spacings and crack widths do not decrease in the same manner. The maximum contribution of fibres is reached at high strain levels, which frequently lie above the elastic range of bar reinforcement. The results, obtained for a fibre content of only 0.9 vol.-%, confirm that in combination with bar reinforcement, the fibre concrete itself does not need to show strain hardening behaviour to achieve progressive crack formation with very small crack spacings and crack widths, which enables very durable structures. Since the costs of the fibres mainly determine the costs of UHPC, this finding is of high economical importance.

Model ideas developed so far, which primarily suggest a superposition of the load-deformation-behaviour of fibre concrete and stress-strain-relationship of plain steel without considering compatibility (e.g. [5]) are not able to reproduce this observation.

6 References

[1] Fehling, E.; Schmidt, M.; Teichmann, Th.; Bunje, K.; Bornemann, R.; Middendorf, B.: Entwicklung, Dauerhaftigkeit und Berechnung Ultra-Hochfester Betone (UHPC). In: Forschungsbericht DFG FE 497/1-1, Structural Materials and Engineering Series, no. 1, Kassel University, 2005.

[2] RILEM 1970, Technical Recommendations for the Testing and Use of Construction Materials: RC 6, Bond Test for Reinforcement Steel, 2. Pull-out Test, 1970.

[3] Pfyl, Th.: Tragverhalten von Stahlfaserbeton. PhD Thesis, ETH Zürich, 2003.

[4] Leutbecher, T.: Rissbildung und Zugtragverhalten von mit Stabstahl und Fasern bewehrtem Ultrahochfesten Beton (UHPC). PhD Thesis, Kassel University, 2007.

[5] Jungwirth, J.: Zum Zugtragverhalten von zugbeanspruchten Bauteilen aus Ultra-Hochleistungs-Faserbeton. PhD Thesis N° 3429 (2006), École Polytechnique Fédérale de Lausanne, 2006.